

ASTERIX - A Shallow Water Equation type model for hydrodynamic process on hillslope. Water flow modulus.

Stelian Ion*, Dorin Marinescu*, Stefan-Gicu Cruceanu*

Abstract

The hillslope hydrological processes represent one of the most important problem in watershed hydrology research. Our focus in this report is oriented towards the water flow on the soil surface in a hydrographic basin. In order to obtain quantitatively estimations of some physical variables (e.g. water depth and water velocity), we proceed as follows. First, based on general principles of fluid mechanics, we introduce a PDE model. Using finite volume method for approximating the spatial derivatives, we build an ODE system which constitutes the base of the discrete model we will work with.

Keywords: hydrological process, balance equations, shallow water equations, finite volume method, well balanced scheme, energy conservation.

1 Introduction

Mathematical modeling of the hydrodynamic processes in hydrographic basins is a very active research area due to at least the following two main reasons, in our opinion: the subject is very reach in the practical applications and there

*“Gheorghe Mihoc-Caius Iacob” Institute of Mathematical Statistics and Applied Mathematics, Romanian Academy, 050711 Bucharest, Romania, email: stelian.ion@ima.ro, dorin.marinescu@ima.ro, stefan.cruceanu@ima.ro.

Supported by the Grant 50/2012 ASPABIR funded by Executive Agency for Higher Education, Research, Development and Innovation Funding, Romania (UEFISCDI).

is not yet a satisfactory model to enhance the entire complexity of these processes. However, there are plenty of models, each of them been performant to some specific facets of the hydrodynamic processes. To review the existent mathematical models is beyond this paper, but we can group them into two large classes: physical base models and regression models. The most known regression models are the unit hydrograph [13] and universal soil loss [14, 15]. From the first class, we mention here a few well known models: SWAT [17], SWAP [18], and KINEROS [16].

Due to the complexity and heterogeneity of the processes [12], models in the physical base class are not pure physical based ones, but they also need some empirical relations. The main difference between different models is given by the nature of the empirical relations. For example, SWAP and KINEROS models use a mass balance equation and a closure relation to model the surface water flow, while SWAT model combines the one dimensional mass balance equation with the momentum balance equation to model the surface water flow.

A very special class of models are cellular automata. Such models combine in a specific way microscale physical laws with empirical closure relations to build up a macroscale model, e.g. CAESAR [20, 21].

The model we introduce in the paper belongs to the class of physical base models. Based on general principles of fluid mechanics and using a space average method, we obtain a shallow water type equation model. This model takes into consideration topography, water-soil and water-plant interactions. To integrate the model, we use finite volume method for approximating the spatial derivatives and a type of fractional time-step method to gain the evolution of the water depth and velocity field.

After introducing the PDE model in Section 2, we perform the Finite Volume Method (FVM) approximation in Section 3 and obtain an ODE version of Shallow Water Equation (SWE). We then investigate some physical relevant qualitative properties of this ODE system: monotonicity of the energy, positivity of the water depth function h , well balanced properties of the scheme. In Section 5 we obtain the full discrete variant of our continuous model; we tackle on method validation and give some numerical results in the last section.

2 Shallow Water Equations

The model we discuss here is a simplified version a more general model of water flow on a hillslope introduced in [5]. One assumes that the soil surface is represented by

$$x^3 = z(x^1, x^2), \quad (x^1, x^2) \in \Omega,$$

and that the first derivatives of the function $z(\cdot, \cdot)$ are small quantities. The unknown variables of the model are the water depth $h(t, x)$ and the two components $v_a(t, x)$, $a = 1, 2$ of the water velocity \mathbf{v} , while the density of the plant cover is quantified by a porosity function $\theta(x)$. The model reads as

$$\begin{aligned} \partial_t \theta h + \partial_a (\theta h v^a) &= \mathfrak{M}, \\ \partial_t (\theta h v_a) + \partial_b (h v_a v^b) + \theta h \partial_a w &= -\mathcal{K}(h, \theta) |\mathbf{v}| v_a, \quad a = 1, 2. \end{aligned} \quad (1)$$

The term $\mathcal{K}(h, \theta) |\mathbf{v}| v_a$ quantifies the interactions water- soil and water-plants [1, 11], and the function $\mathcal{K}(h, \theta)$ is given by

$$\mathcal{K}(h, \theta) = \alpha_p h (1 - \theta) + \theta \alpha_s, \quad (2)$$

where α_p and α_s are two characteristic parameters of the strength of the water-plant and water-soil interactions, respectively. The contribution of the rain and infiltration to the water mass balance is taken into account by the function \mathfrak{M} . Also, $w = g [z(y^1, y^2) + h]$ in (1) stands for the free surface level, and g for the gravitational acceleration.

It is important to note that there exists an energy function \mathcal{E} given by

$$\mathcal{E} := \frac{1}{2} |\mathbf{v}|^2 + g \left(x^3 + \frac{h}{2} \right) \quad (3)$$

that obeys a conservative equation

$$\partial_t (\theta h \mathcal{E}) + \partial_a \left(\theta h v^a \left(\mathcal{E} + g \frac{h}{2} \right) \right) = \mathfrak{M} \left(-\frac{1}{2} |\mathbf{v}|^2 + w \right) - \mathcal{K} |\mathbf{v}|^3. \quad (4)$$

In the absence of the mass source, the system preserves the steady state of a lake

$$\partial_a (x^3 + h) = 0, \quad v_a = 0, \quad a = 1, 2. \quad (5)$$

The model (1) is a hyperbolic system of equations with source term, see [4].

When developing our approximation scheme, we wish among other things that the numerical solutions to preserve the lake, and the scheme to be

well balanced and energetic conservative. These last two properties of a numerical algorithm for shallow water equation are very important, especially for the case of hydrographic basin applications, because they allow the lake formation and prevent the numerical solution to oscillate in the vicinity of a lake. In the absence of porosity, there are many proposals of such schemes, see [3, 6, 10] for example.

3 FVM approximation of 2D model

Let Ω be the domain of the space variables and let $\Omega = \cup_i \omega_i, i = \overline{1, N}$ be an admissible polygonal partition of it, [7]. To build a spatial discrete approximation of the model (1), one integrates the continuous equations on each finite volume ω_i and then defines an approximation of the integrals.

Let ω_i be an arbitrary element of the partition. Relatively to it, the integral form of (1) reads as

$$\begin{aligned} \partial_t \int_{\omega_i} \theta h dx + \int_{\partial \omega_i} \theta h \mathbf{v} \cdot \mathbf{n} ds &= \int_{\omega_i} \mathfrak{M} dx, \\ \partial_t \int_{\omega_i} \theta h v_a dx + \int_{\partial \omega_i} \theta h v_a \mathbf{v} \cdot \mathbf{n} ds + \int_{\omega_i} \theta h \partial_a w dx &= - \int_{\omega_i} \mathcal{K} |\mathbf{v}| v_a dx, \quad a = 1, 2. \end{aligned} \quad (6)$$

We now build up a discrete version of the integral form by introducing some quadrature formulas. Let ψ_i stand for some approximation of ψ on ω_i . First, we introduce the approximations

$$\int_{\omega_i} \theta h dx \approx \sigma_i \theta_i h_i, \quad \int_{\omega_i} \theta h v_a dx \approx \sigma_i \theta_i h_i v_{ai}, \quad \int_{\omega_i} \mathcal{K} |\mathbf{v}| v_a dx \approx \sigma_i \mathcal{K}_i |\mathbf{v}|_i v_{ai}, \quad (7)$$

where σ_i denotes the area of the polygon ω_i .

Concerning the integrals of the gradient of the free surface, we start from the identity

$$\int_{\omega_i} \theta h \partial_a w dx = - \int_{\omega_i} w \partial_a \theta h dx + \int_{\partial \omega_i} w \theta h n_a ds,$$

and then approximate the first integral on the r.h.s. by considering w constant and equal to w_i to obtain

$$\int_{\omega_i} \theta h \partial_a w dx \approx \int_{\partial \omega_i} (w - w_i) \theta h n_a ds. \quad (8)$$

Note that if ω_i is a regular polygon and w_i is the cell-centered value of w , then the approximation is of second order accuracy for smooth fields and preserves the null value in the case of constant fields w .

We introduce the notation

$$\widetilde{\psi}|_{\partial\omega(i,j)} := \int_{\partial\omega(i,j)} \psi ds.$$

Using the approximations (7) and (8) and keeping the boundary integrals, one writes

$$\begin{aligned} \sigma_i \partial_t \theta_i h_i + \sum_{j \in \mathcal{N}(i)} \widetilde{\theta h v_n}|_{\partial\omega(i,j)} &= \sigma_i \mathfrak{M}_i, \\ \sigma_i \partial_t \theta_i h_i v_{ai} + \sum_{j \in \mathcal{N}(i)} \widetilde{\theta h v_a v_n}|_{\partial\omega(i,j)} + \sum_{j \in \mathcal{N}(i)} (w - w_i) \widetilde{\theta h n_a}|_{\partial\omega(i,j)} &= -\sigma_i \mathcal{K}_i |\mathbf{v}|_i v_{ai}, \end{aligned} \quad (9)$$

where $\mathcal{N}(i)$ denotes the set of all the neighbors of ω_i and $\partial\omega(i,j)$ is the common boundary of the ω_i and ω_j .

The next step is to define the approximations of the boundary integrals. We approximate an integral on a side $\partial\omega(i,j)$ by considering the integrand to be a constant function of the two adjacent cell values ω_i and ω_j

$$\begin{aligned} \widetilde{\theta h v_n}|_{\partial\omega(i,j)} &\approx l_{(i,j)} \theta h_{(i,j)} (v_n)_{(i,j)}, \\ \widetilde{\theta h v_a v_n}|_{\partial\omega(i,j)} &\approx l_{(i,j)} \theta h_{(i,j)} (v_a)_{(i,j)} (v_n)_{(i,j)}, \\ (w - w_i) \widetilde{\theta h n_a}|_{\partial\omega(i,j)} &\approx l_{(i,j)} (w_{(i,j)} - w_i) \theta h_{(i,j)}^s n_a^{(i,j)}, \end{aligned} \quad (10)$$

where $\mathbf{n}_{(i,j)}$ denotes the unitary normal to the common side of ω_i and ω_j pointing towards ω_j , and $l_{(i,j)}$ is the length of this common side.

The issue is to define the interface value functions $\psi_{(i,j)}(\psi_i, \psi_j)$ such that the scheme will be well balanced and energetic stable.

Well balanced and energetic stable scheme. For any internal interface (i,j) , let us define the following quantities:

$$\begin{aligned} (v_a)_{(i,j)} &= \frac{v_{ai} + v_{aj}}{2}, \quad a = 1, 2, \\ (v_n)_{(i,j)} &= \mathbf{v}_{(i,j)} \cdot \mathbf{n}^{(i,j)}, \\ w_{(i,j)} &= \frac{w_i + w_j}{2}, \end{aligned} \quad (11)$$

and

$$\theta h_{(i,j)}^s = \begin{cases} \theta h_{(i,j)}, & \text{if } (v_n)_{(i,j)} \neq 0, \\ \theta_i h_i, & \text{if } (v_n)_{(i,j)} = 0 \text{ and } w_i > w_j, \\ \theta_j h_j, & \text{if } (v_n)_{(i,j)} = 0 \text{ and } w_i \leq w_j. \end{cases} \quad (12)$$

We remark that there exists one degree of freedom in the way we define the θh values on these internal interfaces.

h -positivity. In order to preserve the positivity of h we define $\theta h_{(i,j)}$ as

$$\theta h_{(i,j)} = \begin{cases} \theta_i h_i, & \text{if } (v_n)_{(i,j)} > 0, \\ \theta_j h_j, & \text{if } (v_n)_{(i,j)} < 0. \end{cases} \quad (13)$$

We can now build the semidiscrete scheme as the following system of ODEs

$$\begin{aligned} \sigma_i \frac{d}{dt} \theta_i h_i + \sum_{j \in \mathcal{N}(i)} l_{(i,j)} \theta h_{(i,j)} (v_n)_{(i,j)} &= \sigma_i \mathfrak{M}_i, \\ \sigma_i \frac{d}{dt} \theta_i h_i v_{ai} + \sum_{j \in \mathcal{N}(i)} l_{(i,j)} \theta h_{(i,j)} (v_a)_{(i,j)} (v_n)_{(i,j)} + \\ + \frac{1}{2} \sum_{j \in \mathcal{N}(i)} l_{(i,j)} (w_j - w_i) (\theta h)_{(i,j)}^s n_a|_{(i,j)} &= -\sigma_i \mathcal{K}_i |\mathbf{v}|_i v_{ai}, \end{aligned} \quad (14)$$

with the quantities defined in (11), (12) and (13).

Boundary conditions. Free discharge. To define the values of h and v on the external sides of the finite volume, we introduce a new volume (“ghost” element) adjacent to the partition of the domain. For each such external element, one can define its altitude and then we set zero values to its water depth. For the element inside the domain Ω and adjacent to the boundary $\Gamma = \partial\Omega$, we extend the velocity up the external boundary of the element,

$$\begin{aligned} \mathbf{v}_{\partial\omega_i \cap \Gamma} &= \mathbf{v}_i, \\ h_{\partial\omega_i \cap \Gamma} &= \begin{cases} h_i, & \text{if } v_i \cdot n|_{\partial\omega_i \cap \Gamma} > 0, \\ 0, & \text{if } v_i \cdot n|_{\partial\omega_i \cap \Gamma} < 0. \end{cases} \end{aligned} \quad (15)$$

Now, the solution is sought inside the positive cone $h_i > 0$, $i = \overline{1, N}$.

4 Properties of the semidiscrete scheme

The ODE model (14) may have discontinuities in the r.h.s. This fact implies that the solution in the classical sense of this system may not exist for some

initial data. However, the solution in Filipov sense [19] exists for any initial data.

There are initial data for which the solution in the classical sense exists locally in time. Since the numerical scheme is a time approximation of the semidiscrete form (14), we think it will be worthwhile to analyze the properties of these classical solutions.

4.1 Energy balance

The interface value definition (11) yields a dissipative conservative equation for the cell energy \mathcal{E}_i ,

$$\mathcal{E}_i(h_i, \mathbf{v}_i) = \theta_i \left(\frac{1}{2} |\mathbf{v}_i|^2 h_i + \frac{1}{2} g h_i^2 + g x_i^3 h_i \right). \quad (16)$$

The time derivative of \mathcal{E}_i can be written as

$$\sigma_i \frac{d\mathcal{E}_i}{dt} = \sigma_i \left(\left(w_i - \frac{1}{2} |\mathbf{v}_i|^2 \right) \frac{d\theta_i h_i}{dt} + \left\langle \mathbf{v}_i, \frac{d\theta_i h_i \mathbf{v}_i}{dt} \right\rangle \right), \quad (17)$$

where $\langle \cdot, \cdot \rangle$ denotes the euclidean scalar product in \mathbb{R}^2 .

Proposition 4.1 (Cell energy equation) *In the absence of mass source one has*

$$\sigma_i \frac{d}{dt} \mathcal{E}_i + \sum_{j \in \mathcal{N}(i)} l_{(i,j)} \langle \mathcal{H}_{(i,j)}, n_{(ij)} \rangle = -\sigma_i \mathcal{K}_i |\mathbf{v}_i|^3, \quad (18)$$

where

$$\mathcal{H}_{(i,j)} = \frac{1}{2} \theta h_{(i,j)} (w_i \mathbf{v}_i + w_j \mathbf{v}_j + \langle \mathbf{v}_i, \mathbf{v}_j \rangle \mathbf{v}_{(i,j)}).$$

Remark 4.1 *One notes that if $(\theta h, v, w)_j = (\theta h, v, w)_i$ for any $j \in \mathcal{N}(i)$ then*

$$\mathcal{H} = \theta h \mathbf{v} \left(\frac{1}{2} |\mathbf{v}|^2 + w \right),$$

which is the continuous flux energy in (4).

Proof. Using the equality (17), one can write

$$\begin{aligned}\sigma_i \frac{d}{dt} \mathcal{E}_i &= -(w_i - \frac{1}{2} |\mathbf{v}_i|^2) \sum_{j \in \mathcal{N}(i)} l_{(i,j)} \theta h_{(i,j)}(v_n)_{(i,j)} - \\ &\quad - \left\langle \mathbf{v}_i, \sum_{j \in \mathcal{N}(i)} l_{(i,j)} \theta h_{(i,j)} \mathbf{v}_{(i,j)} (v_n)_{(i,j)} \right\rangle - \\ &\quad - \frac{1}{2} \left\langle \mathbf{v}_i, \sum_{j \in \mathcal{N}(i)} l_{(i,j)} (w_j - w_i) (\theta h)_{(i,j)}^s \mathbf{n}_{(i,j)} \right\rangle - \\ &\quad - \sigma_i \mathcal{K}_i |\mathbf{v}_i|^3.\end{aligned}$$

Now, one has the identities

$$\begin{aligned}w_i \sum_{j \in \mathcal{N}(i)} l_{(i,j)} \theta h_{(i,j)}(v_n)_{(i,j)} &= \sum_{j \in \mathcal{N}(i)} l_{(i,j)} \theta h_{(i,j)}(v_n)_{(i,j)} \frac{w_i + w_j}{2} + \\ &\quad + \sum_{j \in \mathcal{N}(i)} l_{(i,j)} \theta h_{(i,j)}(v_n)_{(i,j)} \frac{w_i - w_j}{2},\end{aligned}$$

and

$$\begin{aligned}&\left\langle \mathbf{v}_i, \sum_{j \in \mathcal{N}(i)} l_{(i,j)} (w_j - w_i) (\theta h)_{(i,j)}^s \mathbf{n}_{(i,j)} \right\rangle = \\ &= \sum_{j \in \mathcal{N}(i)} l_{(i,j)} (w_j - w_i) (\theta h)_{(i,j)}^s \left\langle \frac{\mathbf{v}_i + \mathbf{v}_j}{2} + \frac{\mathbf{v}_i - \mathbf{v}_j}{2}, \mathbf{n}_{(i,j)} \right\rangle,\end{aligned}$$

and therefore

$$\begin{aligned}w_i \sum_{j \in \mathcal{N}(i)} l_{(i,j)} \theta h_{(i,j)}(v_n)_{(i,j)} + \frac{1}{2} \left\langle \mathbf{v}_i, \sum_{j \in \mathcal{N}(i)} l_{(i,j)} (w_j - w_i) (\theta h)_{(i,j)}^s \mathbf{n}_{(i,j)} \right\rangle &= \\ &= \sum_{j \in \mathcal{N}(i)} l_{(i,j)} \theta h_{(i,j)} \langle w_i \mathbf{v}_i + w_j \mathbf{v}_j, \mathbf{n}_{(i,j)} \rangle.\end{aligned}$$

Similarly, one obtains the identity

$$\begin{aligned}-\frac{1}{2} |\mathbf{v}_i|^2 \sum_{j \in \mathcal{N}(i)} l_{(i,j)} \theta h_{(i,j)}(v_n)_{(i,j)} + \left\langle \mathbf{v}_i, \sum_{j \in \mathcal{N}(i)} l_{(i,j)} \theta h_{(i,j)} \mathbf{v}_{(i,j)} (v_n)_{(i,j)} \right\rangle &= \\ &= \frac{1}{2} \sum_{j \in \mathcal{N}(i)} l_{(i,j)} \theta h_{(i,j)} \langle \mathbf{v}_i, \mathbf{v}_j \rangle \left\langle \frac{\mathbf{v}_i + \mathbf{v}_j}{2}, \mathbf{n}_{(i,j)} \right\rangle.\end{aligned}$$

If we take out the mass exchange through the boundary, then the interface values imply the monotonicity of the energy with respect to time.

4.2 h-positivity and critical points

Proposition 4.2 (h-positivity) *The ODE system (14) with (11),(12) and (13) preserves the positivity of the water depth function h .*

Proof. One can rewrite the mass balance equations as

$$\sigma_i \frac{d}{dt} \theta_i h_i = -(\theta h)_i \sum_{j \in \mathcal{N}(i)} l_{(i,j)} (v_n)_{(i,j)}^+ + \sum_{j \in \mathcal{N}(i)} l_{(i,j)} (\theta h)_j (v_n)_{(i,j)}^-,$$

and observe that if $h_i = 0$ for some i then $\sigma_i \frac{d}{dt} \theta_i h_i \geq 0$.

There are two kinds of stationary points for the ODE model: the lake and uniform flow on an infinitely extended plan with constant vegetation density.

Proposition 4.3 (Stationary point. Uniform flow.) *Let $\{\omega_i\}_{i=\overline{1,N}}$ be a regular partition of Ω with ω_i being a regular poligon, and $z - z_0 = \xi_b x^b$ be a representation of the soil plane surface. Assume that the discretization of the soil surface is given by*

$$z_i - z_0 = \xi_b \bar{x}_i^b, \quad (19)$$

where \bar{x}_i^b is the mass center of the ω_i , and that $\theta_i = \theta$. Then, given a value h , there exist values v^a such that the state $h_i = h$ and $v_i^a = v^a$ is a stationary point of ODE (14).

Proof. For any constant state $h_i = h$ and $v_i^a = v^a$, the ODE (14) is reducing to

$$\frac{1}{2} \theta h g \sum_{j \in \mathcal{N}(i)} l_{(i,j)} (z_j - z_i) n_a|_{(i,j)} = -\sigma \mathcal{K} |v| v_a.$$

Introducing the representation (19), one writes

$$\frac{1}{2} \theta h g \sum_{j \in \mathcal{N}(i)} l_{(i,j)} \xi_b (\bar{x}_j^b - \bar{x}_i^b) n_a|_{(i,j)} = -\sigma \mathcal{K} |v| v_a.$$

One notes that for a regular partition there exists the identity

$$\bar{x}_j^b - \bar{x}_i^b = 2(y_{(i,j)} - \bar{x}_i^b),$$

where $y_{(i,j)}$ is the midpoint of the common side $\bar{\omega}_i \cap \bar{\omega}_j$. Taking into account that

$$\begin{aligned}
\frac{1}{2}\theta hg \sum_{j \in \mathcal{N}(i)} l_{(i,j)}(z_j - z_i)n_a|_{(i,j)} &= \theta hg \sum_{j \in \mathcal{N}(i)} l_{(i,j)}\xi_b y_{(i,j)}^b n_a|_{(i,j)} \\
&= \theta hg \int_{\partial\omega_i} \xi_b x^b(s) n_a(s) ds \\
&= \theta hg \int_{\omega_i} \xi_b \partial_a x^b dx \\
&= \sigma \theta hg \xi_a.
\end{aligned}$$

one obtains that the velocity is a constant field and equals to

$$v_a = \xi_a \left(\frac{\theta hg}{\mathcal{K}|\xi|} \right)^{1/2} \quad (20)$$

A lake is a stationary point characterized by constant values of the free surface and null velocity field on connex regions. A lake for which $h_i > 0$ for any $i \in \{1, \dots, N\}$ will be named *regular stationary point* and a lake that occupies only a part of a domain flow will be named *singular stationary point*.

Proposition 4.4 (Stationary point. Lake.) *The following holds:*

(a) *Regular stationary point. In the absence of mass source, the state $w_i = w$, $\mathbf{v}_i = 0$, $i = \overline{1, N}$ is a stationary point of the ODE.*

(b) *Singular stationary point. In the absence of mass source, the state $\mathbf{v}_i = 0$, $i = \overline{1, N}$, $w_i = w$, $i \in \mathcal{I}$, $h_i = 0$, $z_i > w$, $i \in \mathbf{CI}$ is a stationary point.*

Proof. For the case of the singular stationary point, it is interesting to consider that the set $\Omega_{\mathcal{I}} = \cup_{i \in \mathcal{I}} \omega_i$ is a connex domain. Since the velocity field is zero, the only thing one has to verify is that for any cell ω_i we have

$$\sum_{j \in \mathcal{N}(i)} l_{(i,j)}(w_j - w_i)(\theta h)_{(i,j)}^s n_a|_{(i,j)} = 0.$$

If i belongs to \mathbf{CI} (the complement of \mathcal{I}), then the sum equals zero since $h_{(i,j)}^s = 0$ for all $j \in \mathcal{N}(i)$. If i belongs to \mathcal{I} then sum is again zero because either $h_{(i,j)}^s = 0$ for $j \in \mathbf{CI}$ or $w_j = w_i$ for $j \in \mathcal{I}$.

5 Fractional Step-time Schemes

In what follows we discuss different explicit or semi-implicit schemes to integrate the ODE (14).

Let us introduce some notations

$$\begin{aligned}\mathcal{J}_{ai}(h, v) &:= - \sum_{j \in \mathcal{N}(i)} l_{(i,j)} \theta h_{(i,j)} (v_a)_{(i,j)} (v_n)_{(i,j)}, \\ \mathcal{S}_{ai}(h, w) &:= - \frac{1}{2} \sum_{j \in \mathcal{N}(i)} l_{(i,j)} (w_j - w_i) (\theta h)_{(i,j)}^s n_a|_{(i,j)}, \\ \mathcal{L}_i((h, v)) &:= - \sum_{j \in \mathcal{N}(i)} l_{(i,j)} \theta h_{(i,j)} (v_n)_{(i,j)}.\end{aligned}\tag{21}$$

The ODE model (14) is written as

$$\begin{aligned}\sigma_i \frac{d}{dt} \theta_i h_i &= \mathcal{L}_i(h, v) + \sigma_i \mathfrak{M}(t, h), \\ \sigma_i \frac{d}{dt} \theta_i h_i v_{ai} &= \mathcal{J}_{ai}(h, v) + \mathcal{S}_{ai}(h, w) - \mathcal{K}(h) |\mathbf{v}_i| v_{ai}.\end{aligned}\tag{22}$$

Source mass. We assume that the source mass \mathfrak{M} can be written as

$$\mathfrak{M}(x, t, h) = r(t) - \theta(x) \iota(t, h),\tag{23}$$

where $r(t)$ quantifies the rate of the rain and $\iota(t, h)$ quantifies the infiltration rate. The infiltration rate is a continuous function and satisfies the following

$$\iota(t, h) < \iota_m, \text{ if } h \geq 0.\tag{24}$$

The basic idea of a fractional time method is to split the initial ODE into two sub-models, integrate them separately, and then combine the two solutions [8, 9].

We split the ODE (14) as the follows:

$$\begin{aligned}\sigma_i \frac{d}{dt} \theta_i h_i &= \mathcal{L}_i(h, v), \\ \sigma_i \frac{d}{dt} \theta_i h_i v_{ai} &= \mathcal{J}_{ai}(h, v) + \mathcal{S}_{ai}(h, w),\end{aligned}\tag{25}$$

and

$$\begin{aligned}\sigma_i \frac{d}{dt} \theta_i h_i &= \sigma_i \mathfrak{M}_i(t, h), \\ \sigma_i \frac{d}{dt} \theta_i h_i v_{ai} &= -\mathcal{K}(h) |\mathbf{v}_i| v_{ai}.\end{aligned}\tag{26}$$

A first order fractional step time accuracy reads as

$$\begin{aligned}\sigma(\theta h)^* &= \sigma(\theta h)^n + \Delta t_n \mathcal{L}((h, v)^n), \\ \sigma(\theta h v_a)^* &= \sigma(\theta h v_a)^n + \Delta t_n (\mathcal{J}_a((h, v)^n) + \mathcal{S}_a((h, w)^n)),\end{aligned}\quad (27)$$

$$\begin{aligned}\sigma(\theta h)^{n+1} &= \sigma(\theta h)^* + \sigma \Delta t_n \mathfrak{M}(t^{n+1}, h^{n+1}), \\ \sigma(\theta h v_a)^{n+1} &= \sigma(\theta h v_a)^* - \Delta t_n \mathcal{K}(h) |\mathbf{v}^{n+1}| v_a^{n+1}.\end{aligned}\quad (28)$$

The two steps (27) and (28) lead to

$$\begin{aligned}\sigma(\theta h)^{n+1} &= \sigma(\theta h)^n + \Delta t_n \mathcal{L}((h, v)^n) + \sigma \Delta t_n \mathfrak{M}(t^{n+1}, h^{n+1}), \\ \sigma(\theta h v_a)^{n+1} &= \sigma(\theta h v_a)^n + \Delta t_n (\mathcal{J}_a((h, v)^n) + \mathcal{S}_a((h, w)^n)) - \\ &\quad - \Delta t_n \sigma \mathcal{K}(h) |\mathbf{v}^{n+1}| v_a^{n+1}.\end{aligned}\quad (29)$$

To advance a time step, one needs to solve a scalar nonlinear equation for h and a 2D nonlinear system of equations for velocity \mathbf{v} .

It is important to analyze the physical properties of the numerical solution given by (29). In what follows, we investigate the h-positivity, the well balanced property and the monotonicity of the energy.

5.1 h-positivity. Stationary points

Proposition 5.1 (h-positivity) *There exists an upper bound τ_n for the time step Δt_n such that if $\Delta t_n < \tau_n$ and $h^n > 0$ then $h^{n+1} \geq 0$.*

Proof. For any cell i one has

$$\begin{aligned}\sigma_i \theta_i h_i^{n+1} + \Delta t_n \iota(t^{n+1}, h_i^{n+1}) &= \sigma_i \theta_i h_i^n \left(1 - \frac{\Delta t_n}{\sigma_i} \sum_{j \in \mathcal{N}(i)} l_{(i,j)} (v_n)_{(i,j)}^{n,+} \right) + \\ &\quad + \Delta t_n \sum_{j \in \mathcal{N}(i)} l_{(i,j)} (\theta h^n)_j (v_n)_{(i,j)}^{n,-} + \Delta t_n r(t^{n+1}).\end{aligned}$$

The upper bound τ_n is given by

$$t_n < \frac{1}{v_{\max}^n} \min_i \left\{ \frac{\sigma_i}{\sum_{j \in \mathcal{N}(i)} l_{(i,j)}} \right\}. \quad (30)$$

Proposition 5.2 (Well balanced) *The lake and the uniform flow are stationary points of the scheme (29).*

Proof. Similar to the propositions 4.3 and 4.4.

Unfortunately the semi-implicit scheme does not preserve the monotonicity of the energy.

5.2 Discrete energy

Let us rewrite the energy amount between two consecutive steps as

$$\begin{aligned}
\mathcal{E}^{n+1} - \mathcal{E}^n &= \sum_i \theta_i \sigma_i (h_i^{n+1} - h^n) (w_i^n - \frac{|v_i^n|^2}{2}) + \\
&+ \sum_i \theta_i \sigma_i \langle (h\mathbf{v})_i^{n+1} - (h\mathbf{v})_i^n, \mathbf{v}_i^n \rangle + \\
&+ g \sum_i \theta_i \sigma_i \frac{(h_i^{n+1} - h^n)^2}{2} + \sum_i \theta_i \sigma_i \frac{h_i^{n+1}}{2} |\mathbf{v}_i^{n+1} - \mathbf{v}_i^n|^2.
\end{aligned} \tag{31}$$

If the sequence $(h, \mathbf{v})^n$ is given by (29) one obtains

$$\begin{aligned}
\mathcal{E}^{n+1} - \mathcal{E}^n &= -\Delta t_n \sum_i \sigma_i \mathcal{K}(h^{n+1}) |\mathbf{v}_i^{n+1}|^2 \langle \mathbf{v}_i^{n+1}, \mathbf{v}_i^n \rangle + \\
&+ g \sum_i \theta_i \sigma_i \frac{(h_i^{n+1} - h^n)^2}{2} + \sum_i \theta_i \sigma_i \frac{h_i^{n+1}}{2} |\mathbf{v}_i^{n+1} - \mathbf{v}_i^n|^2 + \\
&+ TS + TB,
\end{aligned} \tag{32}$$

where TB and TS stand for the contribution of boundary and mass source to the energy production.

One can now see that the scheme adds energy at each time step. We also observe that the scheme introduces spurious oscillations in the vicinity of the lake points. To decrease the amount of energy added by the semi-implicit scheme (29) and to eliminate these oscillation, we introduce artificial viscosity in the scheme [7, 22]. Adding a “viscous” contribution to the term \mathcal{J} ,

$$\mathcal{J}_{ai}^v = \mathcal{J}_{ai}(h, v) + \sum_{j \in \mathcal{N}(i)} l_{(i,j)} \nu_{(i,j)} ((v_a)_j - (v_a)_i), \tag{33}$$

the amount of energy is now given by

$$\mathcal{E}_v^{n+1} - \mathcal{E}_v^n = \mathcal{E}^{n+1} - \mathcal{E}^n - \Delta t_n \sum_{s(i,j)} l_{(i,j)} \nu_{(i,j)} |\mathbf{v}_i - \mathbf{v}_j|^2, \tag{34}$$

which indicates a dissipation of the energy.

5.3 Stability

The stability of any numerical scheme ensures that errors in data at a step-time are not further amplified along the next steps. To acquire the stability

of our scheme, we have investigated several time-bounds τ_n and different formulas for the viscosity ν . The best results were obtained by the following choice:

$$\tau_n = \frac{\phi_{\min}}{c_{\max}^n}, \quad \nu_{(i,j)} = (\theta h)_{(i,j)} c_{(i,j)}, \quad (35)$$

where

$$\begin{aligned} c_i &= |\mathbf{v}|_i + \sqrt{gh_i}, \\ c_{\max} &= \max_i \{c_i\}, \\ c_{(i,j)} &= \max\{c_i, c_j\}, \\ \phi_{\min} &= \min_i \left\{ \frac{\sigma_i}{\sum_{j \in \mathcal{N}(i)} l_{(i,j)}} \right\}. \end{aligned} \quad (36)$$

Remark 5.1 *An upper bound as (35) for the time-step is well known in the theory of hyperbolic system, CFL condition [2, 7].*

6 Validation

A rough classification of validation methods splits them into two classes: internal and external. For the internal validation, one analyses the numerical results into a theoretical frame: comparison to analytical results, sensibility to the variation of the parameters, robustness, stability with respect to the errors in the input data etc. These methods validate the numerical results with respect to the mathematical model and not with the physical processes; this type of validation is absolutely necessary to assure the mathematical consistency of the method.

The external validation methods assume a comparison of the numerical data with real data measured in the field. The main advantage of them is that a good consistency of data validates both the numerical data and the mathematical model. In the absence of measured data, one can do a qualitative analysis: the evolution given by the numerical model is similar to the observed one, without pretending quantitative estimations.

6.1 Internal validation

We are comparing numerical results given by a 1-D version of our model with the analytical solution for a Riemann problem. Figure 1 shows a very good

agreement when the porosity is constant and a good one when the porosity (cover plant density) varies. Also, in Figure 2 we analyze the response of our

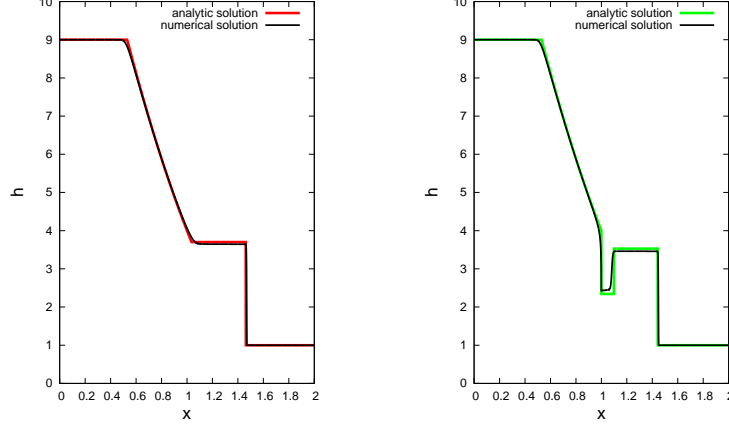


Figure 1: Comparison of the numerical and analytical solutions for the Riemann Problem. The surface is described by $z = 1$ and at the initial moment we have: velocity field $\mathbf{v} = \mathbf{0}$, and there is a discontinuity in the water-depth h : $h = 9$ for $x < 1$, $h = 1$ for $x > 1$. Left picture - constant porosity: $\theta = 1$. Right picture - variable porosity: $\theta = 0.8$ for $x < 1$, $\theta = 1$ for $x > 1$.

model to the variation of the parameters.

6.2 External validation

Unfortunately, we do not have data for the water distribution, plant cover density and measured velocity field in a hydrographic basin to compare our numerical results with. However, to be closer to reality, we have used GIS data for the soil surface of Paul's Valley and accomplished a theoretical experiment: starting with a uniform water depth on the entire basin and using different cover plant densities, we run our model, ASTERIX. Figure 2 shows that the numerical results are consistent with direct observations concerning the water time residence in the hydrographic basin.

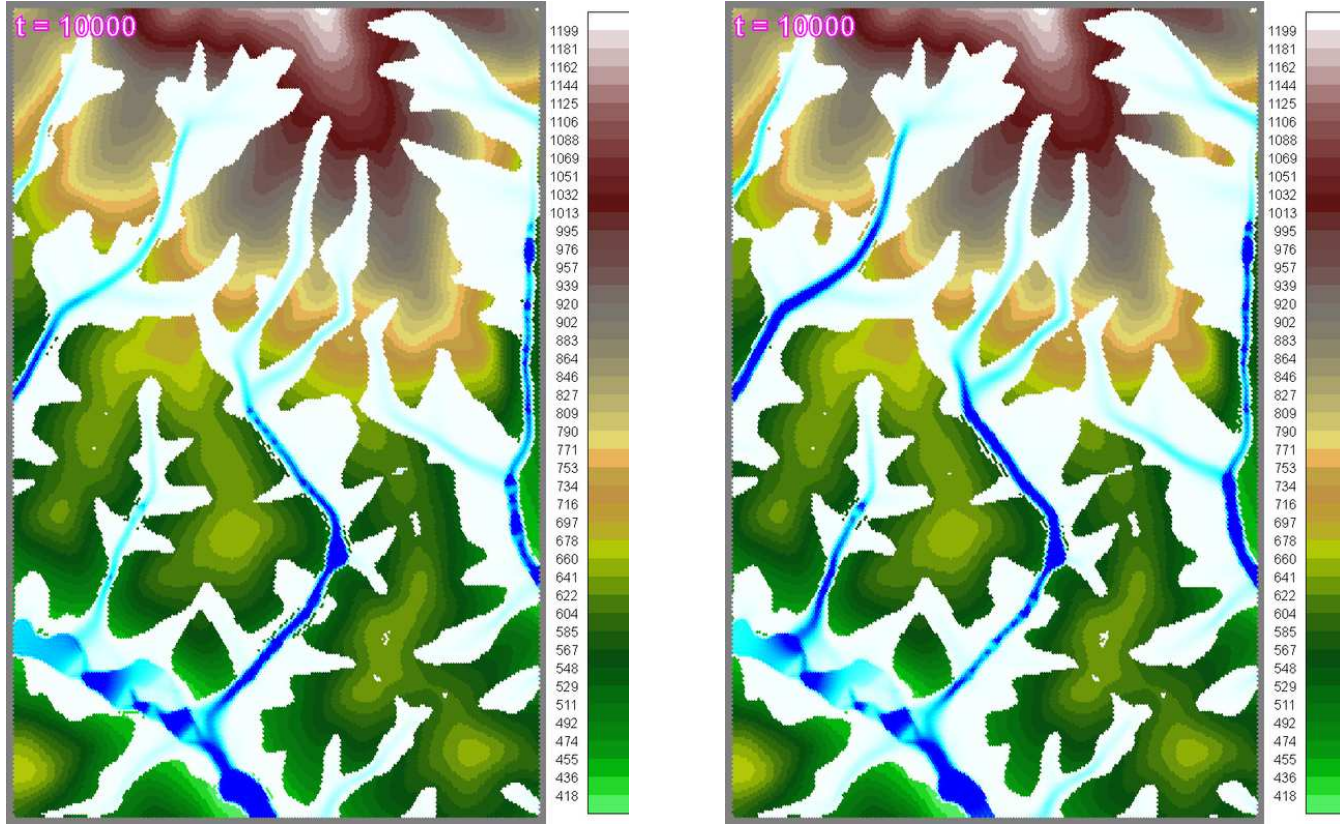


Figure 2: Snapshot of water distribution in Paul's Valley hydrographic basin. Direct observations indicate that the water time residence depends on the density of the cover plant. Our numerical data are consistent with terrain observations: the water drainage time is bigger for the case of higher cover plant density. $\theta = 3\%$ and $\theta = 35\%$ for the left and right picture, respectively.

Figure 3 shows the results for the water content in Paul’s Valley basin obtained with our models ASTERIX and CAESAR-Lisflood-OSE. This variable q is in fact the relative amount of water in the basin at the moment of time t :

$$q(t) = \frac{\int_{\Omega} h(t, x) dx}{\int_{\Omega} h(0, x) dx}.$$

This variable is also a measure of the amount of water leaving the basin.

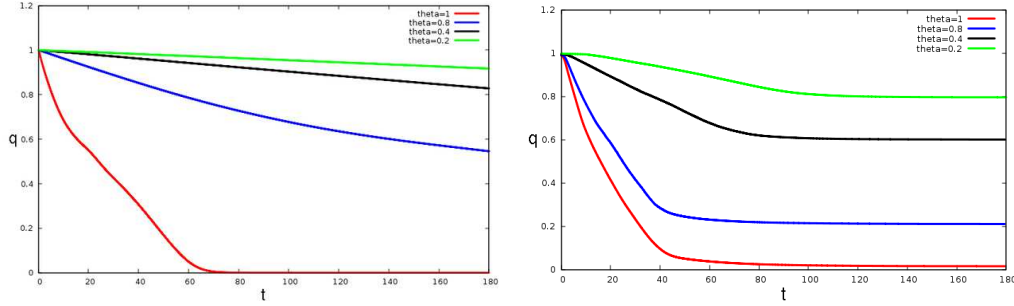


Figure 3: Time evolution of the water content in Paul’s Valley hydrographic basin with ASTERIX (left picture) and CAESAR (right picture).

A general issue relates to the problem if higher cover plant densities can prevent soil erosion and flood. Both pictures show that if the cover plant density is increasing then the decreasing rate \dot{q} of q is smaller. We can think at a “characteristic velocity” of the water movement in the basin and this velocity is in a direct relation with \dot{q} . We can now speculate that smaller values of \dot{q} imply softer erosion processes.

This valley belongs to Ampoi’s catchment basin. Flood generally appears when the discharge capacity of a river is overdue by the water coming from the river catchment area. Our pictures show that higher cover plant densities imply smaller values of \dot{q} which in turn give Ampoi River the time to evacuate the water amount flowing from the valley.

References

- [1] M.J. Baptist, V. Babovic, J. Rodriguez Uthurburu, M. Keijzer, R.E. Uittenbogaard, A. Mynett and A. Verwey, *On inducing equations for*

- vegetation resistance*, Journal of Hydraulic Research, **45**:4(2007), pp. 435–450.
- [2] F. Bouchut, *Nonlinear Stability of Finite Volume Methodes for Hyperbolic Conservation Laws*, Birkhauser, 2004.
 - [3] A. Chinnayya, A.Y. LeRoux, N. Seguin, *A well-balanced numerical scheme for the approximation of the shallow-water equations with topography: the resonance phenomenon*, International Journal on Finite Volume (electronic), volume 1(1), pp. 1–33, 2004.
 - [4] Stelian Ion, Dorin Marinescu, Anca- Veronica Ion, Stefan-Gicu Cruceanu, Virgil Iordache, *Water flow on vegetated hill. 1D Shallow water type equation type model*, An. St. Univ. Ovidius, **23**(3),2015, pp. 83–96.
 - [5] S. Ion, D. Marinescu, S.G. Cruceanu, *Overland flow in the presence of vegetation*, Technical report, www.ima.ro/PNII_programme/ASPABIR/pub/report_ismma_aspabir_2013.pdf
 - [6] S. Noelle, N. Pankratz, G. Puppo, J.R. Natvig, *Well-balanced finite volume schemes of arbitrary order of accuracy for shallow water flows*, Journal of Computational Physics, **213** (2006), pp. 474–499.
 - [7] R.L. LeVeque, *Finite Volume Methods foe Hyperbolic Problems*, Cambridge University Press, 2002.
 - [8] R.L. LeVeque, *Time-Split Methods for Partial Differential Equations*, Phd. Thesis, Stanford University, 1982.
 - [9] G. Strang, *On the construction and comparison of difference schemes*, SIAM J. Numer.Anal., 5 (1968), pp. 506-517.
 - [10] U.S. Fjordholm, S. Mishra, E. Tadmor, *Well-balanced and energy stable schemes for the shallow water equations with discontinuous topography*, Journal of Computational Physics, **230** (2011), pp. 5587–5609.
 - [11] H.M. Nepf, *Drag, turbulence, and diffusion in flow through emergent vegetation*, Water Resource Research, **35**: 2(1999), pp. 479–489.

- [12] J. J. McDonnell et al., *Moving beyond heterogeneity and process complexity: A new vision for watershed hydrology*, Water Resour. Res., **43**(2007), W07301, doi:10.1029/2006WR005467.
- [13] James C. I. Dooge, A General Theory of the Unit Hydrograph, Journal of Geophysical Research, **64**(2) (1959), pp. 241-256.
- [14] , Kenneth G. Renard, George R. Foster, Glenn A. Weesies, and Jeffrey P. Porter, *RUSLE Revised universal soil loss equation*, Journal of Soil and Water Conservation, **46**(1), 1991.
- [15] Walter H. Wischmeier, *A Rainfall Erosion Index for a Universal Soil-Loss Equation*, Soil Science Society of America Journal, **23** (3) (1959), pp. 246-249.
- [16] Woolhiser, D.A., Smith, R.E., and Goodrich, D.C., *KINEROS a kinematic runoff and erosion model: documentation and user manual*, ARS-77, U.S. Govt. Printing Ofc., Washinton, D.C.
- [17] , ***, SWAT: Soil and Water Assessment Tool, www.tamu.edu
- [18] ***, SWAP Soil Water Atmosphere Plant, www.swap.alterra.nl
- [19] O. Hajek, Discontinuous differential equations, I, J. Differential Equations, **32**(1979), pp. 149-170.
- [20] ***, Caesar Lisflood Landscape Evolution and Flow Model, <https://sourceforge.net/projects/caesar-lisflood/>
- [21] ***, CAESAR-Lisflood-OSE, www.ima.ro/software/caesat_lisflood_OSE.htm
- [22] Alexander Kurganov, Guergana Petrova, *A second-Order Well-Balanced Positivity Preserving Central-Upwind Scheme for the Saint-Venant System*, Commun. Math. Sci., **5**(1)(2007), pp. 133–160.